PCCP

XPS characterisation of catalysts during production of multiwalled carbon nanotubes

Zoltán Kónya,*[a] János Kiss,[b] Albert Oszkó,[b] Andrea Siska[a] and Imre Kiricsi[a]

[a] *Department of Applied and Environmental Chemistry, University of Szeged, Rerrich Béla tér 1, H-6720 Szeged, Hungary. E-mail: konya@chem.u-szeged.hu*
[b] *Reaction Kinetics Research Group of the Hungarian Academy of Sciences, University of Szeged, P.O. Box 168, H-6701 Szeged, Hungary*

Received 7th September 2000, Accepted 3rd November 2000
First published as an Advance Article on the web 6th December 2000

Characterisation of alumina supported catalysts was performed by TEM and XPS spectroscopy during formation of multiwalled carbon nanotubes from acetylene at 1000 K. TEM images showed that thick carbon fibres (outer diameter is around 20–40 nm) were generated on Fe/Al_2O_3 and Co/Al_2O_3 samples. The only sample producing carbon nanotubes with an average diameter of 8–12 nm was the bimetallic $CoFe/Al_2O_3$. XPS spectra revealed that Fe–Co alloy formed during the interaction of $CoFe/Al_2O_3$ and acetylene at 1000 K.

Introduction

The synthesis of novel materials of nanometre size is one focus of materials science research. Consequently, intense experimental and theoretical effort has been devoted to the preparation, characterisation and application of nanostructures. Carbon nanostructures, particularly carbon nanotubes, are of interest for physical and chemical research since they can be used for hydrogen storage, as potential nanosensors, nanowires and nanoelectrical devices when the interior of the tube is filled with metal, and for polymer fillers.[1]

There are several methods used for the production of carbon nanotubes. These are as follows: electric arc discharge,[2] laser ablation[3] and catalytic vapour deposition (CVD).[4] Using various metals as catalysts supported on zeolite or silica, Ivanov *et al.*,[5] Li *et al.*[6] and Mukhopadhyay *et al.*[7] reported the production of multiwalled carbon tubes with 3–8 nm inner and 5–25 nm outer diameters and up to 60–100 μm length with remarkable efficiency at low temperature. Recently, Laurent *et al.*[8,9] published results on the synthesis of mixture of single-walled nanotubes (SWNTs) and multiwalled nanotubes (MWNTs) at about 1270–1370 K on $Fe–Al_2O_3$ and on $Fe,Co–MgAl_2O_4$ spinels with 2–7% yield. Cobalt and iron supported on alumina[10] could be applied successfully for the synthesis of MWNT carbon nanotubes. There, acetylene was the carbon source. Its decomposition was carried out at atmospheric pressure. The effects of reaction temperature in the range of 770–970 K and of the flow rate of the hydrocarbon were investigated. In a recent study[11] the catalysts were analysed by XRD and UV-VIS spectroscopy, and the surface areas and porosities were determined. Characterisation of carbon nanotubes was performed by electron microscopy. The amount of deposited carbon increased with increasing reaction temperature and the flow rate of acetylene, but decreased with increasing concentration of alumina in the catalyst support. The yield of tube formation was very low at 870 K. High resolution transmission electron microscopic (HRTEM) analysis showed that the outer diameter of the tubes varied from 8 to 26 nm, the tubes were multiwalled, and the number of layers was between 8 and 20.

Although the formation mechanism of MWNTs on heterogeneous catalysts is well documented, some fundamental questions still remain unsolved. They are as follows: (i) What is the nature of interactions between the support and the metal particles? (ii) What is the state of the metal for the bimetallic catalysts? (iii) What sort of alloy formation occurs?

In the present paper we focus on the characterisation of the chemical state of the catalyst before and after acetylene treatments by *in situ* XPS method.

Experimental

I. Preparation of the catalyst

Alumina was synthesised from aluminium isopropoxide (Aldrich). About 100 g of aluminium isopropoxide powder was spread over a wet filter in a Petri dish and slowly hydrolysed completely using distilled water. The $Al(OH)_3$ gel thus obtained was aged at ambient temperature overnight and then placed in a hot air oven at 313 K for 24 h. The dry solid was ground into a fine powder. For preparation of cobalt supported alumina, 10 g alumina was wetted with 10 ml of aqueous solution of cobalt(II)-acetate. The mixture was homogenised thoroughly and placed in a hot air oven at 313 K for 24 h. The solids were then ground into a fine powder. The Co/Al_2O_3 catalyst had 2.5% cobalt after pretreatment. The iron supported alumina was prepared using iron(II) acetate solution following the procedure used in the preparation of Co supported samples. The Fe/Al_2O_3 sample contained 2.5% iron. Cobalt–iron supported alumina catalyst was prepared in a similar way to that described above. A mixture of iron and cobalt acetate solution was used for wetting the material. The sum of the metal content was 2.5%.

II. Synthesis and *in situ* characterisation of the catalysts by XPS

The XPS experiments were performed in an ultra-high vacuum system with a background pressure of 10^{-9} mbar, produced by an iongetter pump. The photoelectrons generated by Al Kα primary radiation (15 kV, 15 mA) were analysed with a hemispherical electron energy analyser (Kratos XSAM 800). The pass energy was set to 40 eV. An energy step width of 50 meV and a dwell time of 300 ms were used. Typically 10 scans were accumulated for each spectrum.

Fitting and deconvolution of the spectra were performed with the help of VISION software. All binding energies were referenced to Al(2p) at 74.7 eV.

Before measurements, the sample was evacuated at 300 K and calcined at 1000 K for 20 min in the sample preparation chamber, which was connected directly to the analysing chamber by a sample transfer system. In the sample preparation chamber the catalyst can be heated up to 1100 K in various gas atmospheres (in the present case in acetylene–nitrogen mixture).

III. Characterisation of the obtained carbon materials

The various stages of carbon nanotube formation were studied by transmission electron microscopy (TEM). For analysis the samples were prepared by sonicating ~1 mg of synthesised sample in 10 ml ethanol. A few drops of the resulting suspension were then put onto a holey-carbon TEM grid. Both low- (Phillips CM20) and high-resolution (JEOL 200CX) TEM analyses have been made.

Results and discussion

I. XPS spectroscopy

(a) Catalyst Fe/Al_2O_3. After evacuation of as-received Fe/Al_2O_3, $Fe(2p_{1/2})$ and $Fe(2p_{3/2})$ were monitored. The emission of $2p_{3/2}$ appeared at 711.6 eV, as the $2p_{1/2}$ was measured at 725.1 eV. The position and energy separation are very close to those observed for FeO(OH) structure.[12] A broad shake-up satellite appeared at 719.8 eV, which is also characteristic of Fe^{3+}. As Fig. 1 shows, both emissions shifted to lower binding energies after 20 min calcination at 1000 K. This indicates that some reduction occurred during heat treatment. When the sintered sample was exposed to acetylene at 300 K the positions of the peaks remained unaltered. In contrast to this treatment, significant changes were observed after the sample was kept at 1000 K in an acetylene atmosphere for 60 min. The $Fe(2p_{3/2})$ signal shifted to lower binding energy by 1.6 eV, and two satellites appeared at around 713.5 and 718.0 eV [Fig. 1(d)]. The most important observation is that in such a strong reducing atmosphere we could not detect photoemission at 707.0 eV, which is characteristic of bulk metal iron. The $2p_{3/2}$ was detected at 708.6 eV. Under this experimental condition partially oxidised iron (such as Fe_xO) should not exist on the catalyst surface. We assume that the higher binding energy indicates that the particle size is small. In the dispersed system neighbouring atoms are fewer than in bulk, and therefore screening electrons are fewer as well. As a consequence, the core-hole screening is less effective and the binding energy of the orbital shifts to higher energy. This effect could operate in the present case, too. However, the large binding energy difference could not be explained only in this way, because 1000 K is a high enough temperature for the agglomeration of iron particles to occur. We are inclined to think that the formation of iron carbide (Fe_2C or Fe_3C) plays an important role in the position of the observed binding energy. Mössbauer spectroscopy may be a good tool for verifying this assumption.

(b) Catalyst Co/Al_2O_3. After evacuation of Co/Al_2O_3 at 300 K, the $Co(2p_{3/2})$ and $Co(2p_{1/2})$ orbitals appeared at 781.55 and 797.40 eV, respectively, and a typical satellite feature was detected at around 787 eV, suggesting an oxide/hydroxide composition. When the catalyst was heated to 1000 K for 20 min, the separation between the two main emissions decreased, and small shifts (0.35 and 0.25 eV, respectively) in their positions were also seen [Figs. 2(a), (b)]. A strong shake-up satellite peak 5 eV higher than its main peak and a spin–orbit coupling of around 15.5 eV indicate the formation of CoO.[13,14]

When the catalyst sintered at 1000 K was exposed to acetylene at 300 K, a new additional photoemission peak appeared for $Co(2p_{3/2})$ at 777.75 eV. The corresponding $2p_{1/2}$ orbital was detected at 792.7 eV [Fig. 2(c)]. More significant changes

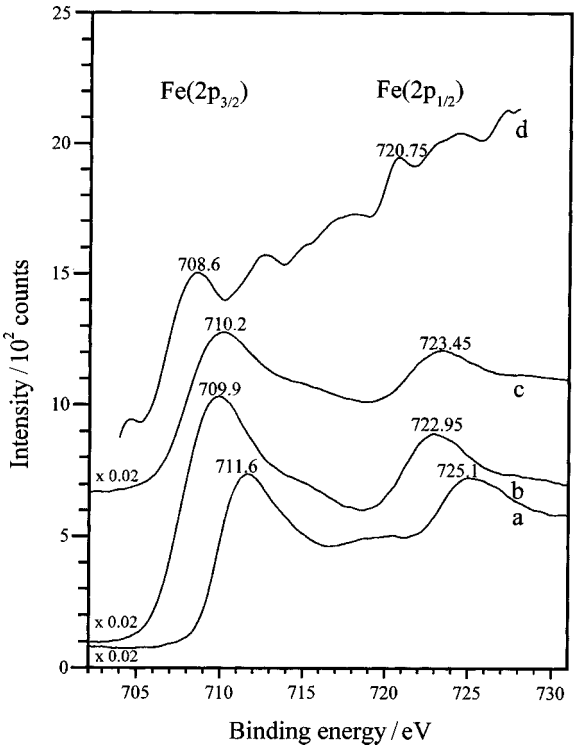

Fig. 1 XP spectra of Fe/Al_2O_3 in Fe(2p) region (a) after evacuation at 300 K for 60 min, (b) after calcination at 1000 K for 20 min, (c) after 20 Torr C_2H_4 adsorption at 300 K for 60 min and (d) after interaction with 20 Torr C_2H_4 at 1000 K for 60 min.

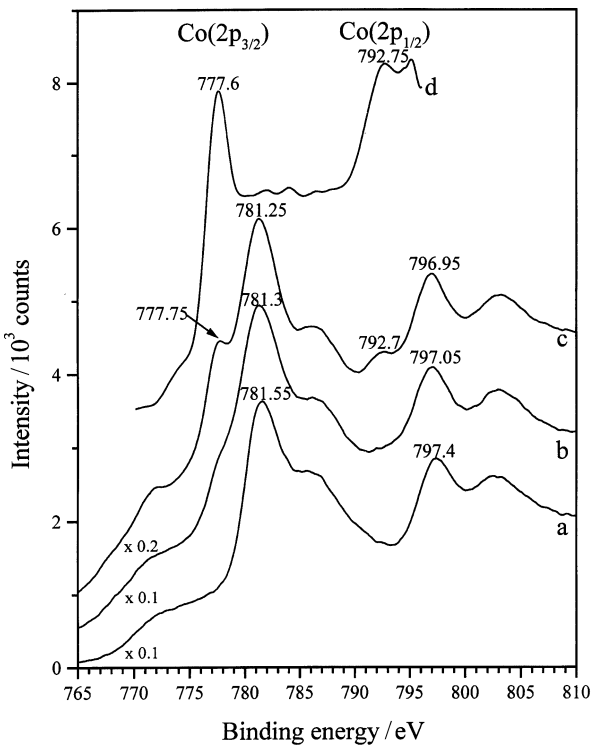

Fig. 2 XP spectra of Co/Al_2O_3 in Co(2p) region (a) after evacuation at 300 K for 60 min, (b) after calcination at 1000 K for 20 min, (c) after 20 Torr C_2H_4 adsorption at 300 K for 60 min and (d) after interaction with 20 Torr C_2H_4 at 1000 K for 60 min.

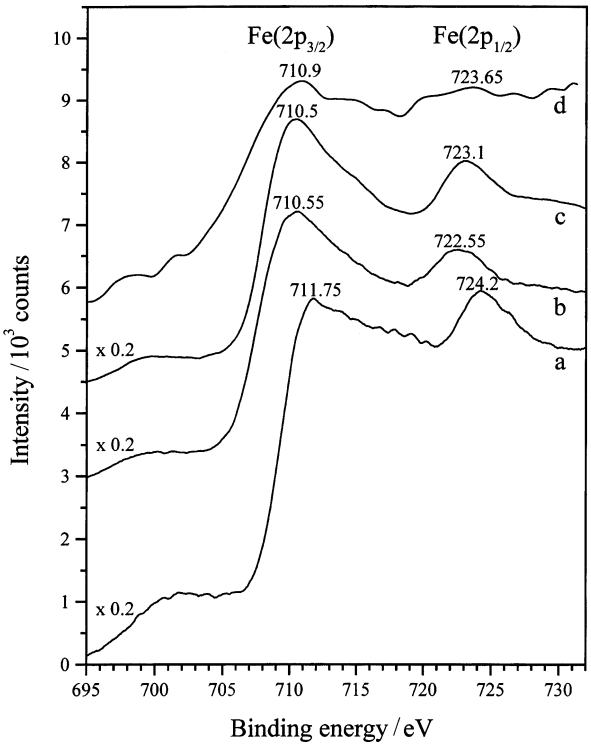

Fig. 3 XP spectra of 5%Fe + 5%Co/Al_2O_3 in Fe(2p) region (a) after evacuation at 300 K for 60 min, (b) after calcination at 1000 K for 20 min, (c) after 20 Torr C_2H_4 adsorption at 300 K for 60 min and (d) after interaction with 20 Torr C_2H_4 at 1000 K for 60 min.

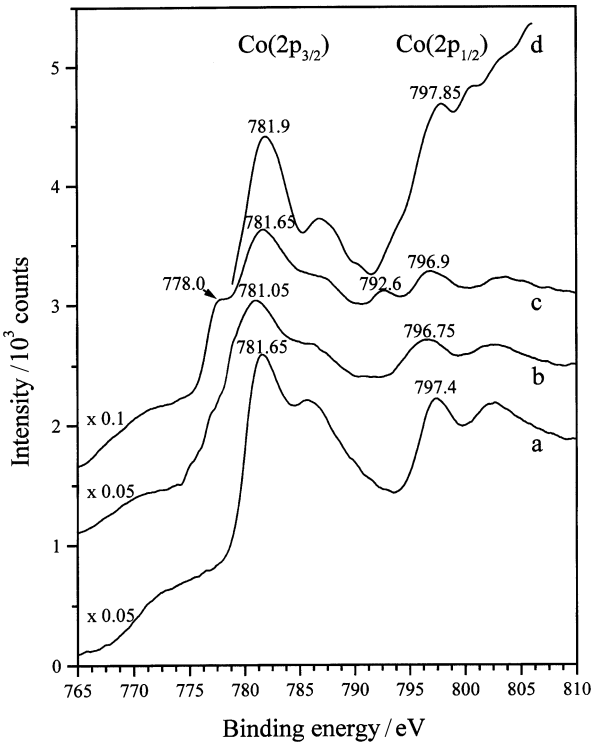

Fig. 4 XP spectra of 5%Fe + 5%Co/Al_2O_3 in Co(2p) region (a) after evacuation at 300 K for 60 min, (b) after calcination at 1000 K for 20 min, (c) after 20 Torr C_2H_4 adsorption at 300 K for 60 min and (d) after interaction with 20 Torr C_2H_4 at 1000 K for 60 min.

were observed when the catalyst was treated in acetylene at 1000 K. All features corresponding to CoO disappeared. Co($2p_{3/2}$) and ($2p_{1/2}$) intensified at 777.6 and 792.75 eV, respectively. These positions and energy separation were measured for metallic cobalt.[15] We also checked the position of carbon after acetylene decomposition. In the case of Co the C(1s) appeared 0.6 eV higher than for the Fe case. If we accept the general picture in the literature, namely that graphitic carbon has higher binding energy than carbidic carbon,[16] we may assume that acetylene decomposition produces mainly graphitic carbon on Co-containing catalyst.

(c) Catalyst FeCo/Al_2O_3. Fig. 3 shows the main photoemission signals of iron in Fe–Co bimetallic catalyst before reduction and after acetylene treatment at 300 and 1000 K. In the unreduced samples (evacuated at 300 K and sintered at 1000 K) the peak positions were almost the same as for Fe/Al_2O_3 [Figs. 3(a), (b)]. It should be noted that the intensities and the shape of the peaks were slightly changed. Acetylene adsorption at 300 K did not cause a significant change. When the bimetallic catalyst was exposed to acetylene at 1000 K, the Fe($2p_{3/2}$) signal moved to higher binding energy by 0.4 eV. The same shift was observed for ($2p_{1/2}$), too. When the Fe was alone in the supported catalyst the direction of the shift was the opposite [Fig. 1(d)]. The formation of small metallic clusters and mainly the formation of Fe_xC may explain the phenomenon. However, in this case we cannot operate with these assumptions. We attribute these changes to the formation of Fe–Co alloy. It is important to mention that a similar shift was observed for Fe–Co/TiO_2 bimetallic catalyst after reduction.[17]

The Co XPS signals were also monitored in the bimetallic system. The presence of Fe caused significant differences in Co(2p) positions in the unreduced sample [Figs. 4(a), (b)]. When this surface was exposed to acetylene at 300 K some portion of cobalt transformed to the reduced state [Fig. 4(c)], which was also observed without iron component [Fig. 2(c)]. In the bimetallic system, there was a drastic change in Co signals when acetylene treatment was carried out at 1000 K. The pure metallic state (778 eV emission) disappeared and a new XPS signal developed at 781.9 eV [Fig. 4(d)]. This value

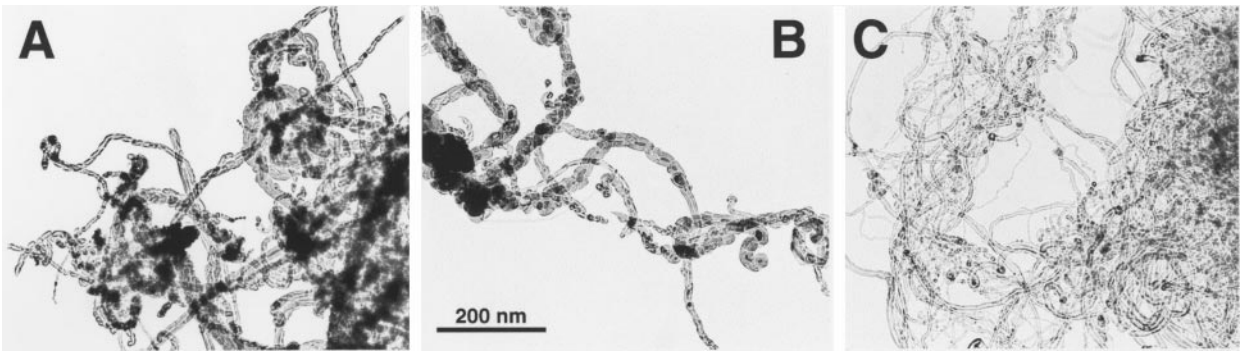

Fig. 5 TEM images of catalyst treated at 1000 K for 20 min in acetylene: Co/Al_2O_3 (A), Fe/Al_2O_3 (B) and CoFe/Al_2O_3 (C).

is higher by 0.9 eV than the measured one for the unreduced, sintered bimetallic system. This positive shift in binding energy of Co also suggests the formation of alloy. This trend was also detected in the case of Fe–Co/TiO_2.[17] The appearance of the metallic state at 300 K transiently indicates that the precursor state of alloy formation is the metallic form.

In order to obtain some information about the large quantity of carbon formed on bimetallic catalyst at 1000 K, the C(1s) peak was also monitored by XPS. The measured 284.65 eV binding energy is higher than that of the carbidic carbon measured on Fe/Al_2O_3. This value is close to that of graphitic carbon, but it is also close to the value measured in the interaction of C_{60} fullerene and carbon nanotube with an Ar ion beam.[18]

II. TEM images

On the catalyst samples treated in *in situ* XPS experiments transmission electron microscopic images were taken in order to reveal the differences between carbon nanostructures formed. Fig. 5 shows three TEM pictures taken on the Fe/Al_2O_3, Co/Al_2O_3 and CoFe/Al_2O_3 samples after *in situ* reaction with acetylene at 1000 K for 20 min. As the pictures show, no tube was formed on supported iron catalyst. The structure on the image is characteristic of carbon fibres. The supported cobalt catalyst behaved similarly. Here again fibres rather than tubes are seen in the picture. The product formed after treatment of CoFe/Al_2O_3 catalyst is completely different from those obtained on monometallic catalysts. Here well-structured carbon nanotubes are seen (Fig. 5C). These images are in agreement with the XPS observations where special carbon formation was proven only on the bimetallic catalyst. TEM images shown here were taken from the same samples that were produced and examined previously in the XPS instrument.

Conclusions

XPS and TEM measurements equally show that carbon nanotube formation only occurred over the bimetallic catalysts. Carbon deposits on the monometallic catalysts were either graphitic or carbidic and carbon fibres were formed predominantly over these catalysts.

Acknowledgements

This work was supported by the grants: OTKA T032040 and FKFP 468/1999. The authors are grateful for this financial assistance.

References

1 P. M. Ajayan, *Chem. Rev.*, 1999, **99**, 1787.
2 Y. Ando and S. Iijima, *Jpn. J. Appl. Phys.*, 1993, **32**, 107.
3 T. Guo, P. Nikolaev, A. Thess, D. T. Colbert and R. E. Smalley, *Chem. Phys. Lett.*, 1995, **243**, 49.
4 V. Ivanov, J. B. Nagy, P. Lambin, A. Lucas, X. B. Zhang, X. F. Zhang, D. Bernaerts, G. Van Tendeloo, S. Amelinckx and J. Van Landuyt, *Chem. Phys. Lett.*, 1994, **223**, 329.
5 V. Ivanov, A. Fonseca, J. B. Nagy, A. Lucas, P. Lambin, D. Bernaerts and X. B. Zhang, *Carbon*, 1995, **33**, 1727.
6 W. Z. Li, S. S. Xie, L. X. Qian, B. H. Chang, B. S. Zhou, W. Y. Zhou, R. A. Zhao and G. Wang, *Science*, 1993, **274**, 1701.
7 K. Mukhopadhyay, A. Koshio, T. Sugai, N. Tanaka, H. Shinohara, Z. Konya and J. B. Nagy, *Chem. Phys. Lett.*, 1999, **303**, 117.
8 C. Laurent, A. Peigney and A. Rousset, *J. Mater. Chem.*, 1998, **8**, 1263.
9 E. Flahaut, A. Govindaraj, A. Peigney, C. Laurent, A. Rousset and C. N. R. Rao, *Chem. Phys. Lett.*, 1999, **300**, 236.
10 J.-F. Colomer, G. Bister, I. Willems, Z. Konya, A. Fonseca, G. Van Tendeloo and J. B. Nagy, *J. Chem. Soc., Chem. Commun.*, 1999, 1343.
11 A. Kukovecz, I. Willems, Z. Konya, A. Siska and I. Kiricsi, *Phys. Chem. Chem. Phys.*, 2000, **2**, 3071.
12 G. C. Allen, M. T. Curtis, A. J. Hooyer and P. M. Tucker, *J. Chem. Soc., Dalton Trans.*, 1974, 1525.
13 B. A. Sexton, A. E. Hughes and T. W. Turney, *J. Catal.*, 1986, **97**, 390.
14 Z. Zsoldos and L. Guczi, *J. Phys. Chem.*, 1992, **96**, 9393.
15 R. Riva, H. Miessner, R. Vitali and G. Del Piero, *Appl. Catal. A*, 2000, **196**, 111.
16 D. A. Wester, G. Linden and H. P. Bonzel, *Appl. Surf. Sci.*, 1986, **26**, 335.
17 D. J. Dunvenhage and N. J. Coville, *Appl. Catal. A*, 1997, **153**, 43.
18 Y. Zhu, T. Yi, B. Zheng and L. Cao, *Appl. Surf. Sci.*, 1999, **137**, 83.